Available online at www.sciencedirect.com
ScienceDirect
Trans. Nonferrous Met. Soc. China 22(2012) 2409−2415

Transactions of Nonferrous Metals Society of China
www.tnmsc.cn

Non-isothermal oxidation and ignition prediction of Ti−Cr alloys

MI Guang-bao[1, 2], HUANG Xiu-song[1], LI Pei-jie[1], CAO Jing-xia[2], HUANG Xu[2], CAO Chun-xiao[2]

1. National Center of Novel Materials for International Research, Tsinghua University, Beijing 100084, China;
2. Aviation Key Laboratory of Science and Technology on Advanced Titanium Alloys, Beijing Institute of Aeronautical Materials, Beijing 100095, China

Received 9 July 2012; accepted 5 August 2012

Abstract: The non-isothermal oxidation behavior and oxide scale microstructure of Ti−Cr alloy ($0\le w(\mathrm{Cr})\le 25\%$) were studied from room temperature to 1723 K by thermogravimetric analysis (TGA), X-ray diffraction (XRD) and scanning electron microscopy (SEM). The influencing mechanism of chromium on the oxidation resistance of Ti−Cr alloys was discussed. The results show that the oxidation resistance of the alloys decreases with Cr below a critical chromium content w_C and increases above w_C; above 1000 K, the oxidation kinetics obeys parabolic rule and titanium dominates the oxidation process; after oxidation, the oxygen-diffusing layer is present in the alloy matrix, the oxide scale is mainly composed of rutile whose internal layer is rich in chromium, and chromium oxides separated out from TiO_2 near the alloy-oxide interface improve the oxidation resistance. Ignition of metals and alloys is a fast non-isothermal oxidation process and the oxidation mechanism of Ti−Cr alloys during ignition is predicted.

Key words: Ti−Cr alloy; non-isothermal oxidation; thermogravimetric analysis (TGA); oxide scale microstructure; ignition

1 Introduction

High thrust−weight ratio is required for next generation of advanced aero-engine, which contradicts the increasing tendency of “titanium fire” of titanium components in compressor. New titanium alloys with high temperature resistance and fire resistance are urgently needed. Fireproof titanium alloys as new high temperature titanium alloys with excellent creep resistance and fire resistance are becoming a promising and critical material for advanced aero-engine [1]. Alloy C (Ti−35V−15Cr) is a highly stable β-type fireproof titanium alloy developed by America and has been used in F119−PW−100 engine for F−22 fighter at the end of last century [2,3]. Until now, “titanium fire” of this alloy has not been reported. Chromium together with vanadium stabilizes β phase, improves the strength and fire resistance of Alloy C, which allows this alloy to work above 800 K [4]. Thus, the effect of chromium on oxidation resistance and fire resistance of titanium alloys attracts attention.

The former researches showed that the oxidation resistance of Ti−Cr alloys decreases below a critical chromium content, while increases above the critical content [4−7]. For example, the oxidation resistance of Ti−Cr alloys at 773−973 K decreases with chromium of 0.5%−8.0% [5]. The oxidation resistance of Ti−Cr alloys at 873−1073 K increases with chromium of 11%−15% [4]. To achieve high fire resistance for Ti−V−Cr alloys, it was proposed by BERCZIK [8] that the chromium content can be 13%−36%. For example, the fireproof alloys Alloy C and Ti40 (Ti−25V−15Cr) contain 15% chromium. LI et al [9] studied the combustion behavior of Ti−35V−15Cr−0.05C, indicating that the glasslike combustion products containing chromium oxides, vanadium oxides and titanium oxides retard the diffusion of species. ZHAO et al [10] studied the combustion behavior of Ti−Cr alloys, concluding that the enrichment of chromium near the interface between alloy and burning products is the reason of improvement of fire resistance, while chromium oxides retard the diffusion of species.

However, most oxidation experiments of titanium alloys containing chromium conducted under isothermal condition and near the working temperature of alloys (<1000 K), which cannot well reveal the effect of chromium on oxidation of titanium alloys containing chromium at higher temperature. Especially, the oxidation mechanism during ignition is still unclear for titanium alloys containing chromium, and effect of chromium on combustion needs further study too. By

Corresponding author: MI Guang-bao; E-mail: miguangbao@163.com; mgb07@mails.tsinghua.edu.cn
DOI: 10.1016/S1003-6326(11)61478-7

TGA, the oxidation characteristics of metals under non-isothermal condition can be obtained. Comparing with combustion, by TGA the oxidation kinetics can be measured precisely in a large temperature range. Meanwhile, comparing with isothermal oxidation, thermogravimetric measurement proceeds quickly, continually and at a higher temperature much more close to combustion temperature, which provides some information about ignition and combustion, especially considering that ignition is a fast non-isothermal oxidation process. For example, TRUNOV et al [11,12] studied the non-isothermal oxidation behavior of aluminum powder, obtained the kinetics parameters and well explained the changeful ignition temperature of aluminum considering phase transformation of alumina. Thus, the high temperature oxidation behavior of Ti−Cr alloys was studied by TGA. Meanwhile, the ignition characteristics were predicted.

2 Experimental

Ti−Cr alloys with chromium content of 0, 5%, 10%, 15%, 20% and 25% by mass were prepared by a 1 kg non-consumable vacuum arc melting furnace. Small pieces of high-purity titanium and chromium were mixed by mass and held in the crucible which was placed in the furnace. After closing the sealing cover of the furnace, the furnace was heated for 20 min, refilled with argon to 1.01×10^5 Pa, then evacuated to 4.0 Pa, and finally refilled with argon of 0.05 Pa. The tungsten electrode was directed to the raw materials and after arc ignition the melting started under the current of 700 A. The blank was inverted after one melting and remelted five times. The ingots were taken out after cooling by a water-cycle system for 30 min. The specimens for oxidation experiments were cut from the centre of the ingots. The surfaces were grinded by 200# and 1000# abrasive papers, then cleaned by acetone and ethanol and dried by flowing air.

The non-isothermal oxidation experiments were conducted on a thermogravimetric analyzer (METTLER TOLEDO TGA/DSC1) with accuracy of 0.01 μg and measuring range from room temperature to 1873 K. An alumina crucible with the inner diameter of 7 mm was used to carry the specimen, which was under a flowing gas mixture of nitrogen (80 mL/min) and oxygen (20 mL/min) during heating. The specimens were heated from room temperature to 1723 K at the heating rate of 20 K/min. Considering the heat release of oxidation, the highest experimental temperature (1723 K) was lower than the upper temperature limit of the thermogravimetric analyzer (1873 K). However, the mass gain after oxidation is enough to meet the demand of research. For example, the maximum mass gains of Ti−25Cr were 7.5% and 12% for Ti.

Phases of oxide scales were characterized by XRD (Bruker D8 Advance) with scanning speed of 8 (°)/min and step size of 0.02°. Prior to metallographic preparation, the specimens were mounted by resin to avoid the spalling of oxide scales. The specimens were grinded by 200# and 1000# abrasive papers, and polished by diamond paste. Acetone and ethanol were used to clean the specimens, followed with drying by flowing air. Cross-section microstructure was investigated by SEM (JSM−6460LV), coupled with energy dispersive spectroscopy (EDS) for chemical analysis.

3 Results

3.1 Thermogravimetric curves

Figure 1 shows the mass gain curves of Ti−Cr alloys ($0\le w\le25\%$) due to oxidation, obtained after processing the original TGA data. The curves with different chromium contents proceed nearly identically until 1000 K. Above 1100 K, the mass gains of alloys show an obvious difference: the mass gains of Ti−5Cr and Ti−10Cr increase at a similar rate, which is higher than others; the mass gains of Ti and Ti−15Cr increase at a similar rate, which is lower than that of Ti−5Cr or Ti−10Cr; the mass gains of Ti−20Cr and Ti−25Cr are the lowest, which can be obviously observed above 1300 K. As temperature increases, the mass gains of Ti, Ti−5Cr, Ti−10Cr and Ti−15Cr converge, which are respectively 22.95, 24.07, 22.11 and 21.38 mg/cm^2 at 1723 K. At 1723 K, the mass gains of Ti−20Cr and Ti−25Cr are 17.63 and 16.73 mg/cm^2 respectively, showing little difference. As chromium content increases, the visible mass gain starts at a higher temperature. For Ti−25Cr, the starting temperature is 1450 K.

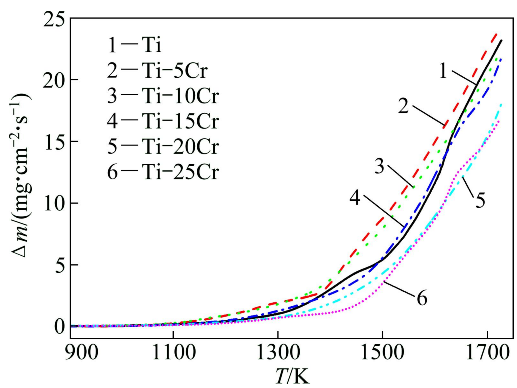

Fig. 1 Mass gain curves of Ti−Cr alloys due to oxidation

In order to investigate the effect of chromium on the non-isothermal oxidation behavior of Ti−Cr alloys quantitively, the oxidation kinetics was processed according to the method first developed for aluminum oxidation [11,12]. The oxidation was assumed to be controlled by a single thermally activated diffusion of one species in the scale. The mass gain rate can be described by the following equation:

$$\frac{\mathrm{d}\Delta m}{\mathrm{d}t}=A\cdot\exp[-E/(RT)]\cdot\frac{1}{\Delta m} \tag{1}$$

where Δm is the mass gain per unit surface area; A is the reaction constant; E is the activation energy; R is the mole gas constant. The heating rate is β in the experiment and $\beta=\mathrm{d}T/\mathrm{d}t$.

The equation (1) can be transformed to

$$\frac{\mathrm{d}\Delta m}{\mathrm{d}T}=\frac{A}{\beta}\cdot\exp[-E/(RT)]\cdot\frac{1}{\Delta m} \tag{2}$$

After logarithmic transformation, the equation is obtained as:

$$-\ln\frac{\mathrm{d}\Delta m}{\mathrm{d}T}-\ln\Delta m=\frac{E}{RT}-\ln\frac{A}{\beta} \tag{3}$$

The left side of Eq. (3) is defined as Y, which can be calculated from TGA data. The relationship between Y and $1000/T$ is shown in Fig. 2. The regions where curves are close to lines with positive slopes are considered valid in terms of the assumption that the oxidation is controlled by a single thermally activated diffusion of one species. For each alloy, the regions at low temperature with negative slopes are considered invalid (Fig. 2(a)). At low temperatures, the mass gain is slow and easy to be disturbed by other factors, such as evaporation of pollutants on the surface. Above 1000 K, for each alloy most regions appear as lines with positive slopes (Fig. 2(b)). Above 1000 K, the severe curve fluctuations are possibly associated with the healing and rupture of oxide scales, which are not considered (Fig. 2(b)). Table 1 shows the oxidation activation energies for the regions considered valid above 1000 K, which are calculated from the slopes of lines. The activation energies for the alloys are 176−282 kJ/mol.

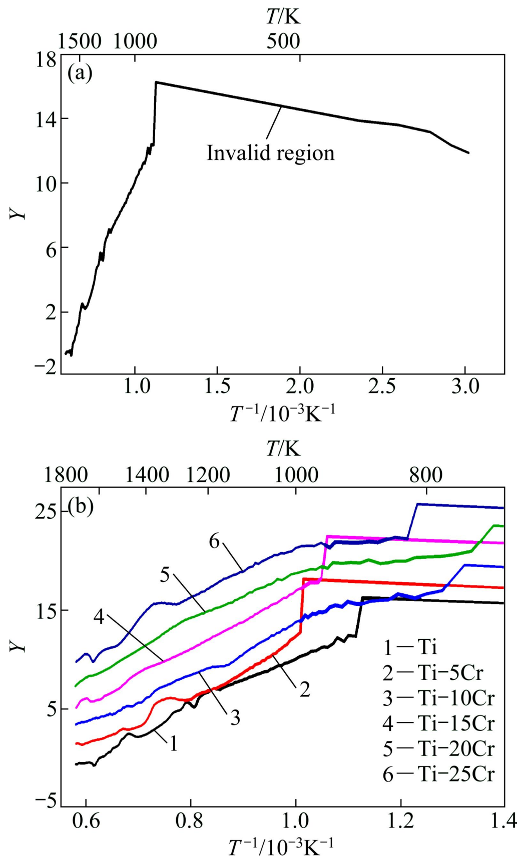

Fig. 2 Relationship between Y and $1000/T$: (a) Ti, in whole measuring temperature range; (b) At high temperature, to show clearly Y of Ti−Cr

Table 1 Oxidation activation energies for regions considered valid above 1000 K

Specimen	Temperature/K	Activation energy/(kJ·mol^{-1})
Ti	934−1223	176
Ti−5Cr	992−1260	265
Ti−10Cr	983−1142	282
Ti−15Cr	973−1434	232
Ti−20Cr	1037−1268	182
Ti−25Cr	1001−1307	202

3.2 Surface analysis

After oxidation, the rupture and breakdown of oxide scales for some alloys were observed. The surface of Ti appears golden red. As chromium content increases, the golden red gradually weakens and the grey gradually intensifies. The surface morphologies of Ti−Cr alloys after oxidation are shown in Fig. 3. The golden red of the oxide scales is obvious for Ti−10Cr, while it disappears for Ti−25Cr, and is replaced with dark grey. The surface of oxide scales is compact.

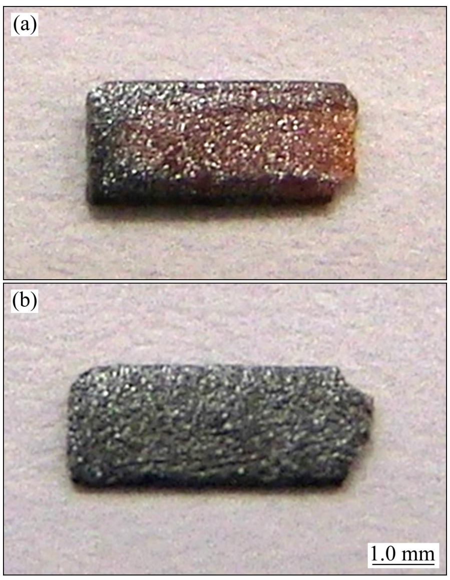

Fig. 3 Surface morphologies of Ti−Cr alloys after oxidation: (a) Ti−10Cr; (b) Ti−25Cr

XRD results of the specimen surfaces after oxidation are shown in Fig. 4. The phases of Ti−Cr alloys are all rutile, the same as the phase of Ti. The chromium oxides are not observed. As the penetration depth of X-ray in TiO_2 (~10 μm) is much smaller than the thickness of oxide scales (>50 μm, see section 3.3), the outer layer of oxide scales is mainly composed of rutile and the inner layer needs further analysis.

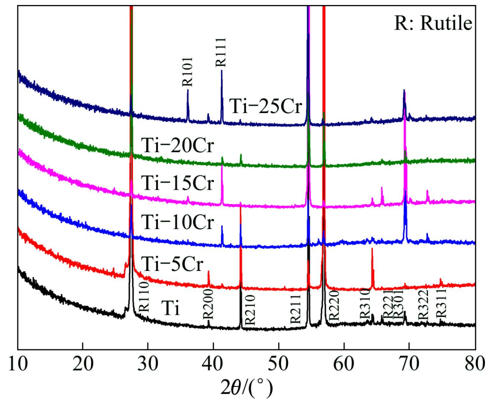

Fig. 4 XRD results of specimen surfaces after oxidation

3.3 Cross-section analysis

SEM and EDS results of Ti−Cr alloys after oxidation are shown in Fig. 5. The oxide scales break away from the alloy (Fig. 5). This is mainly caused by

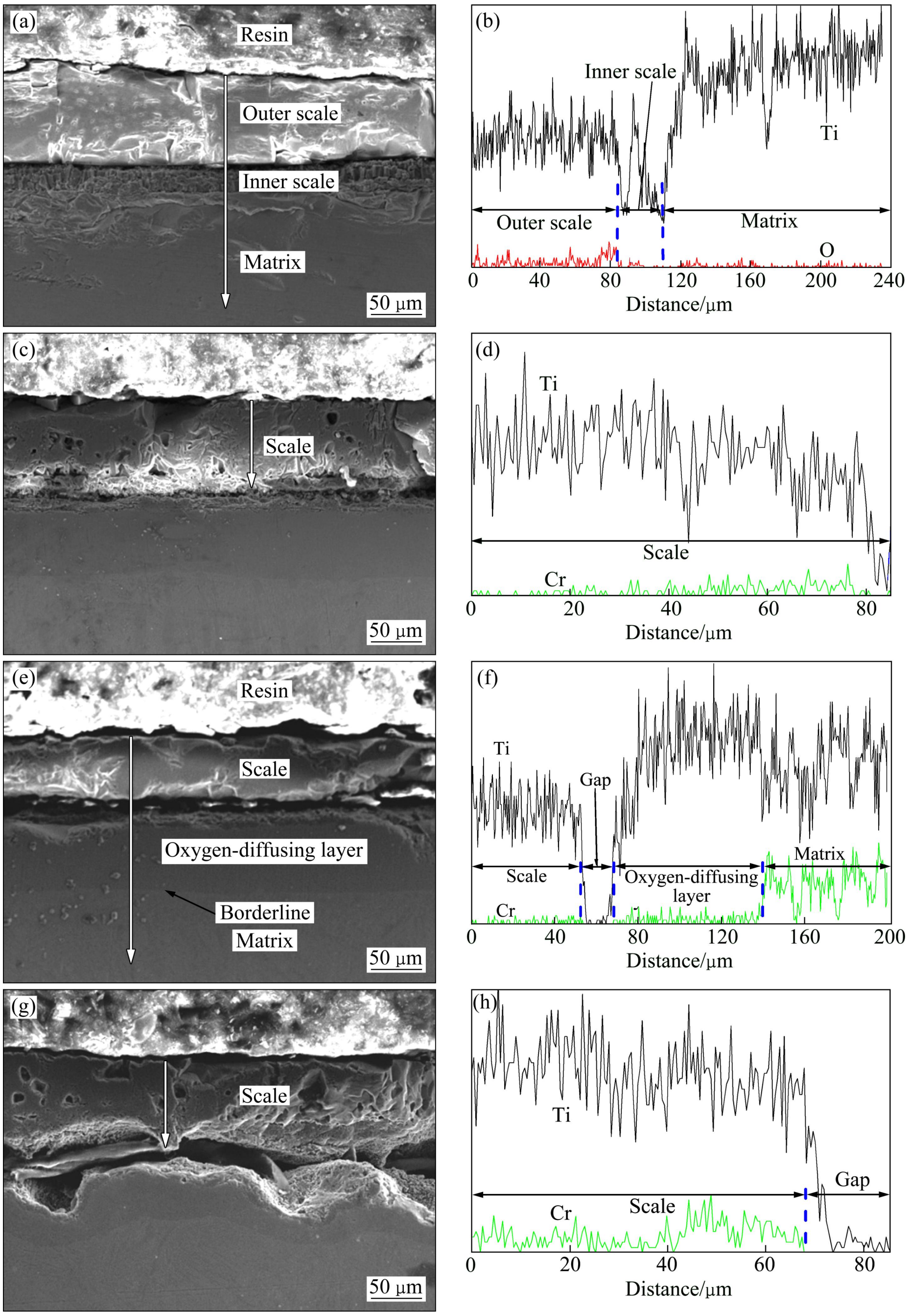

Fig. 5 SEM images and EDS results of Ti−Cr alloys after oxidation: (a), (b) Ti; (c), (d) Ti−15Cr; (e), (f) Ti−20Cr; (g), (h) Ti−25Cr

the thermal stress at the alloy-oxide interface arising during cooling because of the thermal expansion coefficient difference between the alloy and oxide. The oxide scales of Ti are composed of two layers, thick outer layer and thin inner layer closely adhering to the matrix (Fig. 5(a)). For other specimens, the duplex oxide scales are not observed. For Ti−15Cr, Ti−20Cr and Ti−25Cr, the oxygen-diffusing layer is clearly observed, which has a visible borderline compared with the alloy matrix (Figs. 5(c), (e) and (g)). Though the oxide scales contain a large amount of oxygen, the oxygen peaks are weak due to the unsuitability to detect light elements by EDS (Fig. 5(b)). The chromium distributions after oxidation are similar. This characteristic can be represented by Ti−20Cr, with the lowest chromium peaks in the scale, higher peaks in the oxygen-diffusing layer and the highest peaks in the matrix (Fig. 5(f)). The chromium distribution in the scale is also uneven. For Ti−20Cr, dense chromium peaks appear near the alloy-oxide interface (Fig. 5(f)). For Ti−15Cr and Ti−25Cr, the internal layer of the oxide shows higher peaks than the outside layer (Figs. 5(d), (e)).

4 Discussion

According to the thermogravimetric curves, the chromium content has a marked effect on the oxidation resistance of Ti−Cr alloys. The oxidation resistance of Ti−Cr alloys decreases with chromium below a critical chromium content w_C, while increases with chromium above w_C. The critical content in this study is 10%−15%. The changing characteristics of the oxidation resistance with chromium in this study are consistent with the isothermal oxidation results of Ti−Cr alloys at low temperatures, and the critical contents are close. For example, the critical content is around 10% near 873 K by isothermal oxidation experiments [4,5].

Above 1000 K, most regions of curves appear as lines with positive slopes, which indicates that the oxidation kinetics obeys parabolic rule (Fig. 2). The oxidation activation energies for the regions considered valid above 1000 K is 176−282 kJ/mol, close to that of titanium at 873−1123 K (167 kJ/mol [13]) and that of titanium particles obtained by non-isothermal oxidation from 323 to 1473 K (201 kJ/mol [14]). The activation energy is smaller than that of anion diffusion in α-Cr_2O_3 (423 kJ/mol) and larger than that of cation diffusion in α-Cr_2O_3 (92 kJ/mol [15]). In addition, standard free energy of formation of TiO_2 is smaller than that of Cr_2O_3, indicating a higher affinity between titanium and oxygen. The above discussion indicates that titanium dominates the oxidation process and titanium is oxidized first. Two titanium oxides with stable structures can form, which are TiO_2 and TiO. However, the coordination of oxygen close to TiO can only be formed by introducing titanium cation into TiO_2 [16]. Thus, TiO_2 tends to form during oxidation, consistent with the result that phases of oxide scales are mainly rutile by XRD analysis.

Generally, rutile is a n-type semiconductor with high ionic character. In TiO_2, each titanium cation (Ti^{4+}) belongs to six oxygen anions (O^{2-}), constructing TiO_6-octahedron. The Coulomb binding force between anion and cation and the arrange style of TiO_6-octahera determine the stability of the structure [16]. With enrichment of titanium, the coordination number of interstitial titanium cation (Ti_i^{4+}) is also six. The titanium cations are easy to form at the interstitial sites due to a small cation size, and meanwhile the structure of titanium oxides is stable without large lattice distortion. Thus, a large number of interstitial titanium cation point defects appear in TiO_2 [17−19]. Ti_i^{4+} together with oxygen vacancy defect (V_O) forms Schottky defect and a large number of V_O defects exist in the TiO_2 lattice, which is supported by the oxidation results including formation of oxygen-diffusing layer and location of platinum marker [20−23]. As the sizes of Cr^{3+} and Ti^{4+} are close (0.069 and 0.068 nm respectively), Cr^{3+} will replace Ti_i^{4+}, leading to existence of Cr_i^{3+} in TiO_2. During oxidation of Ti−Cr alloys, Ti_i^{4+} diffuses outwards through TiO_2 and captures the inwards diffusing O^{2-}, making the scales grow outwards continually. As a result, the internal layer of oxide scales is rich in chromium, which is consistent with the EDS analysis for oxide scales of Ti−15Cr, Ti−20Cr and Ti−25Cr. Meanwhile, Cr_i^{3+} diffuses outwards and combines with inwards diffusing O^{2-}, forming chromium oxides. However, the diffusing rate of chromium is smaller than that of titanium. In addition, the oxygen-diffusing layer after oxidation indicates the existence of V_O defects and diffusion of O^{2-} through TiO_2. It can be explained as follows. Oxygen diffuses into alloy, forming oxygen-rich area which stabilizes α phase. Compared with the matrix, the phase of oxygen-diffusing layer will not change even the $\alpha\rightarrow\beta$ transformation temperature for pure Ti has been reached. Borderline exists between the matrix and the oxygen-diffusing layer.

Based on the above discussion, the model of microscopic mechanism of oxidation of Ti−Cr alloys above 1000 K was established, as shown in Fig. 6. Three defects V_O, Ti_i^{4+} and Cr_i^{3+} exist in the TiO_2 scales. Ti_i^{4+} has priority over Cr_i^{3+} to diffuse outwards and combines with inwards diffusing O^{2-} forming TiO_2, while Cr_i^{3+} mainly combines with O^{2-} near the alloy-oxide interface to form chromium oxides. The further inward diffusion of oxygen into alloy leads to the oxygen-diffusing layer. At a low chromium content, after Cr_i^{3+} replacing Ti_i^{4+} more V_O defects appear, whose diffusion promotes oxidation. In this range of chromium content, chromium lowers oxidation resistance, corresponding to the oxidation results of Ti−Cr alloys with chromium content lower than 10%. Cr_i^{3+} has a solution limit in TiO_2. For example, at 1673−1923 K, the solution limit of Cr_2O_3 in TiO_2 is 7.5% [24]. Thus, after reaching the solution limit, chromium oxides will separate out from TiO_2, which retard the diffusion of species. In this range of chromium content, chromium improves oxidation resistance, corresponding to the oxidation results of Ti−Cr alloys with chromium content more than 15%.

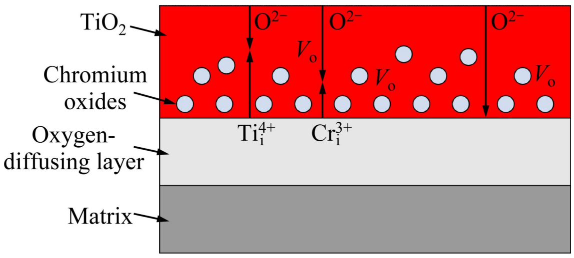

Fig. 6 Microscopic mechanism of oxidation of Ti−Cr alloys

Ignition resistance is a special example of oxidation resistance [25]. Ignition is defined as a chemical reaction under self-accelerated rate and self-increased temperature, accompanied by the production of heat and light. In other words, ignition is a fast self-accelerated non-isothermal oxidation process. Based on this study, it can be predicted that during ignition the alloy-oxide interface of Ti−Cr alloys containing high chromium will be rich in chromium and chromium oxides near the interface will retard the diffusion of species and improve the ignition resistance. The same conclusions can be drawn for other titanium alloys containing chromium. The combustion experiments of Ti−Cr alloys show that the interface between alloy and burning products is also rich in chromium, while no burning resistance shows with chromium lower than 10% [10]. The mechanism of chromium effect on burning resistance of Ti−Cr alloys is similar to that of non-isothermal oxidation. Thus, to some extent, ignition behavior can be predicted by non-isothermal oxidation analysis.

5 Conclusions

1) From room temperature to 1723 K, the oxidation resistance of Ti−Cr alloys is lower than that of Ti below a critical chromium content w_C and increases with chromium content above w_C. The content w_C is 10%−15%. Above 1000 K, the oxidation kinetics obeys parabolic rule.

2) During the non-isothermal oxidation, titanium dominates the process. The oxide scales are mainly composed of rutile. The internal layer of oxide scales is rich in chromium, and oxygen-diffusing layer appears in the matrix.

3) Ti_i^{4+} has priority over Cr_i^{3+} to diffuse outwards, leading to enrichment of chromium in the internal layer of oxide scales. Existence of V_O defects and diffusion of O^{2-} in TiO_2 result in the formation of oxygen-diffusing layer. V_O defects and the oxidation rate of Ti−Cr alloys with a low chromium content increase after Cr_i^{3+} replacing Ti_i^{4+}. With a high chromium content, the separated-out chromium oxides increase the oxidation resistance. The mechanism of the effect of chromium on non-isothermal oxidation of Ti−Cr alloys helps to predict the ignition characteristics of Ti−Cr alloys to some extent.

References

[1] HUANG Xu, LI Zhen-xi, HUANG Hao. Recent development of new high-temperature titanium alloys for high thrust-weight ratio aero-engines [J]. Materials China, 2011, 30(6): 21−27. (in Chinese)

[2] ZHAO Yong-qing, ZHAO Xiang-miao, ZHU Kang-ying. Microstructures of Ti−V−Cr burn resistant titanium alloys [J]. The Chinese Journal of Nonferrous Metals, 1998, 8(3): 463−466. (in Chinese)

[3] HUANG Xu, CAO Chun-xiao, MA Ji-min, WANG Bao, GAO Yang. Titanium combustion in aeroengines and fire-resistant titanium alloys [J]. Journal of Materials Engineering, 1997(8): 11−15. (in Chinese)

[4] HUANG Xu, SUN Fu-sheng, WANG Bao, LI Zhen-xi, CAO Chun-xiao. High temperature oxidation behavior of Ti−Cr alloys [J]. Journal of Aeronautical Materials, 2000, 20(3): 16−20. (in Chinese)

[5] BRODNIKOVSKII N P, ORYSHICH I V, PORYADCHENKO N E, KUZNETSOVA T L, KHMELYUK N D, ROKITSKAYA E A. Resistance of Ti−Cr and zirconium-chromium alloys to air oxidation [J]. Powder Metallurgy and Metal Ceramics, 2010, 49(7−8): 454−459.

[6] XIAO Ping-an, QU Xuan-hui, LEI Chang-ming, ZHU Bao-jun, QIN Ming-li, AO Hui, HUANG Pei-yun. High temperature oxidation behaviors of Ti−Cr alloys with Laves phase $TiCr_2$ [J]. Transactions of Nonferrous Metals Society of China, 2002, 12(2): 200−203.

[7] CHAZE A M, CODDET C. Influence of chromium on the oxidation of titanium between 550 °C and 700 °C [J]. Oxidation of Metals, 1984, 21(3): 205−231.

[8] BERCZIK D M. Age hardenable beta titanium alloy: US Patent 5176762 [P]. 1993−01−05.

[9] LI G P, LI D, LIU Y Y, WANG Q J, GUAN S X, LI Q C. On the burn resistance of Ti−35V−15Cr−0.05C titanium alloys [J]. Acta Metallurgica Sinica, 1998, 11(3): 202−206.

[10] ZHAO Y Q, ZHOU L, DENG J. Effects of the alloying element Cr on the burning behavior of titanium alloys [J]. Journal of Alloys and Compounds, 1999, 284(1−2): 190−193.

[11] TRUNOV M A, SCHOENITZ M, DREIZIN E L. Effect of polymorphic phase transformations in alumina layer on ignition of aluminium particles [J]. Combustion Theory and Modelling, 2006, 10(4): 603−623.

[12] TRUNOV M A, SCHOENITZ M, ZHU X Y, DREIZIN E L. Effect of polymorphic phase transformations in Al_2O_3 film on oxidation kinetics of aluminum powders [J]. Combustion and Flame, 2005, 140(4): 310−318.

[13] GOMES J E L, HUNTZ A M. Comparison of the kinetics and morphologic properties of titanium, Ti−1.5Ni and Ti−2.5Cu during oxidation in pure oxygen between 600 and 820 °C [J]. Oxidation of Metals, 1980, 14(6): 471−498.

[14] SCHULZ O, EISENREICH N, KELZENBERG S, SCHUPPLER H,

NEUTZ J, KONDRATENKO E. Non-isothermal and isothermal kinetics of high temperature oxidation of micrometer-sized titanium particles in air [J]. Thermochimica Acta, 2011, 517(1−2): 98−104.
[15] HAGEL W C. Anion diffusion in alpha-Cr_2O_3 [J]. Journal of the American Ceramic Society, 1965, 48(2): 70−75.
[16] XU Ling, TANG Chao-qun, DAI Lei, TANG Dai-hai, MA Xin-guo. First principles study of the electronic structure of N-doping anatase TiO_2 [J]. Acta Physica Sinica, 2007, 56(2): 1048−1053. (in Chinese)
[17] PENG Li-ping, XIA Zheng-cai, YIN Jian-wu. First-principles calculation of rutile and anatase TiO_2 intrinsic defect [J]. Acta Physica Sinica, 2012, 61(3): 037103. (in Chinese)
[18] HURLEN T. On the defect structure of rutile [J]. Acta Chemica Scandinavica, 1959, 13(2): 365−376.
[19] KOFSTAD P, HAUFFE K, KJOLLESDAL H. Investigation on the oxidation mechanism of titanium [J]. Acta Chemica Scandinavica, 1958, 12(2): 239−266.
[20] UNNAM J, CLARK R K. Oxidation of commercial purity titanium [J]. Oxidation of Metals, 1986, 26(3−4): 231−252.
[21] ROSA C J. Oxygen diffusion in alpha and beta titanium in temperature range of 932 to 1142 ℃ [J]. Metallurgical Transactions, 1970, 1(9): 2517−2521.
[22] STRINGER J. The oxidation of titanium in oxygen at high temperatures [J]. Acta Metallurgica, 1960, 8(11): 758−766.
[23] WALLWORK G R, JENKINS A E. Oxidation of titanium, zirconium, and hafnium [J]. Journal of the Electrochemical Society, 1959, 106(1): 10−14.
[24] SOMIYA S, HIRANO S, KAMIYA S. Phase relations of the Cr_2O_3−TiO_2 system [J]. Journal of Solid State Chemistry, 1978, 25(3): 273−284.
[25] LÜTJERING G, WILLIAMS J C. Titanium [M]. 2nd ed. New York: Springer Berlin Heidelberg, 2007: 51−52.

Ti−Cr 合金的非等温氧化及着火预测

弭光宝 [1,2]，黄秀松 [1]，李培杰 [1]，曹京霞 [2]，黄 旭 [2]，曹春晓 [2]
1. 清华大学 新材料国际研发中心，北京 100084；
2. 北京航空材料研究院 先进钛合金航空科技重点实验室，北京 100095

摘 要：采用热重分析、XRD 和 SEM 等方法研究 Ti−Cr 合金($0\le w(Cr)\le 25\%$)从室温至 1723 K 的非等温氧化行为及氧化膜的微观结构，探讨 Cr 元素对 Ti−Cr 合金抗氧化能力的影响机制。结果表明：当 Cr 含量小于某一临界值 w_C 时，随着 Cr 含量的增加合金的抗氧化能力降低；当 Cr 含量高于 w_C 时，随着 Cr 含量的增加合金的抗氧化能力提高；当温度高到 1000 K 时，Ti−Cr 合金的氧化仍符合抛物线规律，且主要发生钛的氧化；Ti−Cr 合金氧化后基体中存在氧扩散层，氧化膜主要为金红石型 TiO_2，内层氧化膜出现富 Cr 现象，Cr 氧化物的析出提高了 Ti−Cr 合金的抗氧化能力。金属和合金的着火是一个快速非等温氧化的过程，预测了 Ti−Cr 合金着火阶段的氧化机制。

关键词：Ti−Cr 合金；非等温氧化；热重分析；氧化层结构；着火

(Edited by YANG Hua)